Study on the Interference of a Communication System based on a Meta-surface in mmWave

Carola Rizza, Valeria Loscrì

Study on the Interference of a Communication System based on a Meta-surface in mmWave

Carola Rizza
Inria Lille
Lille, 59000 France
carola.rizza@inria.fr

Valeria Loscrí
Inria Lille
Lille, 59000 France
valeria.loscri@inria.fr

***Abstract*—A wireless system in outdoor environment including a reconfigurable intelligent metasurface designed to perform beam-steering is presented. The metasurface unit-cell has been designed to work in the range 37-40 GHz and the designed meta-atom is insensitive to the angle of incidence until 30°. We model and evaluate the effect of interferers on the tracking performances. In particular, we model the channel including interferers and we consider the effect of interferers for different signal powers and different directions on the radiation pattern generated by the metasurface. In general, we notice that the sidelobe level increases when the number of scatterers and their power increase and also when the angle of incidence of the signals scattered from the cluster is increased. Interestingly, for certain configurations, e.g. at $225°$, the radiation pattern at $50°$ is better than at $30°$, showing that the behavior is not linear.**

***Index Terms*—Interferers, beam-steering, meta-surface, mmWave.**

I. Introduction

Recently, there has been an increasing interest on RIM-assisted communication systems, due to their inherent advantages in improving performances and enhancing coverage in an energy-efficient and cost-effective manner [1], [2]. In [3], the path loss models for RIS-assisted wireless communications are developed, but the authors only consider ideal links in line-of-sight between the transmitter/receiver and the RIM. [5] includes mmWave channel models and massive MIMO architectures but it does not take into account the effect of the RIM over the channel. [6] considers RIS-aided millimeter-wave (mmWave) multiple-input multiple-output (MIMO) systems for both accurate positioning and high data-rate transmission but it models the RIS as a uniform linear array (ULA). [7] studies architectures with massive MIMO transmitters that illuminate a large IRS (Intelligent Reflecting Surface) that is dealt as a ULA. Finally, in [8] the authors provide a RIS channel model for mmWave frequencies in presence of interferers. But they don't evaluate the impact of the presence of interferers on the choice of the metasurface phase configuration and so on the generated radiation patterns.

In this paper, we propose a meta-atom, working at mmWave and we consider the metasurface constituted by the periodic repetition of this meta-atom, characterizing its performance for orthogonal impinging signals. We will show that the metasurface is insensitive to the angle of incidence until 30°. The wireless system based on this RIM is applied in an outdoor context and the channel model has been evaluated in presence of scatterers. The system consists of a base station, a reconfigurable intelligent metasurface (RIM) and a mobile receiver. Here only the channel between the base station and the RIM is considered. The base station and the RIM are at the same height and they are aligned in order that the signal transmitted from the base station arrives perpendicularly to the RIM.

In summary, the main contributions of this paper are:

- the design of a reflective 4-state meta-atom in the millimeter wave (37-40 GHz) that is insensitive to the angle of incidence between -30°and 30°;
- the analysis of the interference on the radiation patterns generated by the considered metasurface due to the presence of scatterers in the channel between the base station and the RIM.

Between the base station and the metasurface, there are clusters of scatterers, whose position is random. In this way, the signal transmitted from the base station will be combined with the signals scattered by the interferers, thus creating distortion and deterioration of the signal reflected by the metasurface. Fig.1 shows the considered communication system.

The paper is organized as follows. In Section II the system model is presented by explaining the structure of the designed meta-atom and its behaviour in terms of reflection coefficient. In section III the adopted channel model is discussed. Section IV evaluates the performances of the system in presence of interferers. The paper ends with conclusions in Section V.

II. System model

We consider a scenario in which it is required to send information to a mobile receiver. In order to track the receiver position, a reconfigurable meta-surface with beam-steering capabilities has been adopted. Our meta-surface is tuned by the means of an FPGA (Field-Programmable Gate Array) fed by a unit logic, where we consider a Genetic Algorithm for calculating the new coding scheme of the meta-surface [4]. The meta-surface has been designed in order to perform beam-steering of the impinging signal to a specific direction by tuning the state of each meta-atom. In order to obtain a meta-surface which can steer the direction of the reflected signal in a wide angular range, it is required that each meta-atom has reflective capabilities and that the phase of the

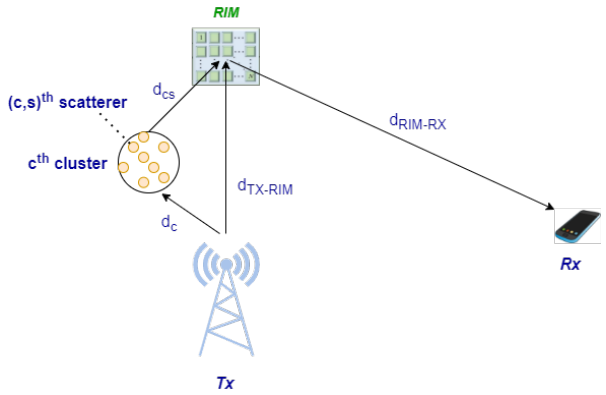

Fig. 1. Channel model of a RIM-assisted system in presence of scatterers.

reflection coefficient has a shift of 90° when the state of the diodes is changed. For this reason, we conceived the meta-atom configuration shown in Fig.2 as unit-cell for this meta-surface, whose working frequency is in the range 37-40 GHz. It consists of a metallic pattern with an irregular shape, over a dielectric substrate and a ground plane. In the metallic pattern, there are two diodes that, together with a via hole placed on the right part of the metallic pattern, make the structure reconfigurable in terms of phase. The via hole connects the metallic pattern upon the substrate to the ground plane.

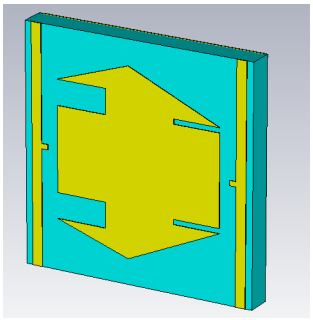

Fig. 2. Meta-atom structure consisting of a metallic pattern, a dielectric substrate (F4B) and a ground plane.

The substrate is made of F4B, whose dielectric constant is 2.65 and the electric tangent loss is 0.001. It has a square shape with each side of length 3.81 mm and its thickness is 0.41 mm. The pattern upon the substrate is made of copper and it has been designed starting from two rectangles of different dimensions with two right-angled triangles of different dimension on both the upper and the lower side. On the obtained structure, 4 cuts have been performed. The diodes have been modeled for simplicity as open circuit for the "off" state and as a short circuit for the "on" state. In the *y* direction two biasing lines have been added in preparation for the entire metasurface made of the repetition of many identical unit-cells, where only the state of the diodes can be modified. This unit-cell has been designed by adopting the "trial and error" approach to obtain the desired features in terms of working frequencies and tuning capability of the

TABLE I
SCATTERING PARAMETERS

		0°	15°	30°	50°	70°	85°
00	mod	0.991	0.989	0.985	0.965	0.87	0.146
00	phase	19.22°	24.25°	39.43°	76.1°	135.22°	-169.28°
01	mod	0.938	0.934	0.922	0.895	0.84	0.783
01	phase	161.25°	164.5°	176.24°	-162.16°	-121.92°	-41.61°
10	mod	0.971	0.969	0.963	0.946	0.868	0.605
10	phase	78.82°	82.04°	93.55°	120.7°	179.87°	-77.15°
11	mod	0.983	0.982	0.98	0.973	0.962	0.978
11	phase	-78.34°	-72.16°	-54.35°	-17.67°	13.44°	7.55°

phase. The aforementioned structure has been simulated on CST (Computer Simulation Technology) [9].
Since a 4-state meta-atom has been chosen for this application, four discrete possible values of the phase can be adopted that are equispaced of 90°. The phase of the reflection coefficients of the four states of the meta-atoms is shown in Fig. 3.

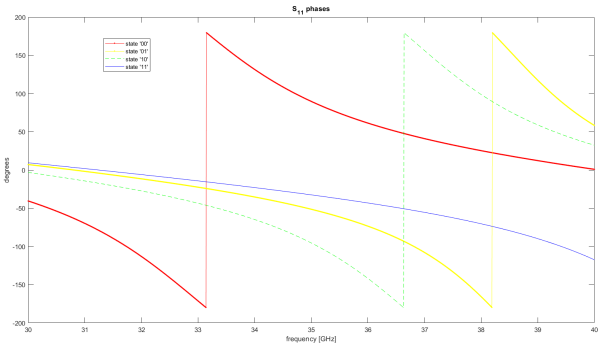

Fig. 3. Phase curve of the S_{11} for the four states of the diode

As it is possible to notice from the graph, the reflection coefficients of the four configurations are shifted of about 90°at frequency f=38.45 GHz.
The behaviour of the meta-atom in terms of reflection coefficient has been evaluated also for different angles of incidence. Table I shows the values of the modulus and of the phase of the reflection coefficients for each state of the meta-atom and for different angles of incidence. As it is possible to notice from the Table I, the phase of the reflection coefficient is acceptable until 30°of incidence. So the metasurface can be illuminated also at angles different from 0°, between -30°and 30°.

III. CHANNEL MODEL

As shown in fig. 1, we consider a wireless system consisting of a transmitter, a RIM and a mobile receiver. Transmitter and RIM are at the same height and they are aligned in order to have the angle of incidence of the signal impinging on the metasurface equal to 0°. Scatterers are considered in the channel between transmitter and metasurface. They are grouped into C clusters, each one with S sub-rays which have the same spatial and/or temporal characteristics. According to [10], the maximum number of clusters that can be chosen for the considered frequency (38.45 GHz) is 2, but here we consider the case of 1 cluster. As regards the number of sub-rays, this number is usually an integer uniformly distributed

between 1 and 30 for the adopted bandwidth [11]. But for simplicity, we assume that the number of sub-rays is fixed to 5, 15 or 30. This assumption does not affect the quality of the results.

For each cluster, the azimuth departure angles $\phi_{c,s}^{TX}$ of the sub-rays are described by a Laplacian distribution whose mean value ϕ_c^{TX} is uniformly distributed *U*[-pi/2,pi/2] and the standard deviation is σ_ϕ= 5° [12]. Also the elevation departure angles $\theta_{c,s}^{TX}$ are conditionally Laplacian with the mean value θ_c^{TX} uniformly distributed *U*[-pi/4,pi/4] and the standard deviation σ_θ= 5° [13]. These departure angles are considered from the transmitter side.

In order to simplify the next computations, all the scatterers belonging to a certain cluster are assumed to be at the same distance d_c from the transmitter. Moreover, d_c is assumed to be uniformly distributed between 1 and d_{TX-RIM}, where d_{TX-RIM} is the LOS link between the transmitter and the metasurface. The distance between each scatterer and the RIM is given by $d_{c,s}$. The distance between TX and RIM d_{TX-RIM} has been computed as:

$$d_{TX-RIM} = ((x^{RIM} - x^{TX})^2 + (y^{RIM} - y^{TX})^2 + (z^{RIM} - z^{TX})^2)^{1/2} \quad (1)$$

where (x^{RIM},y^{RIM},z^{RIM}) and (x^{TX},y^{TX},z^{TX}) are the coordinates of the RIM and of the TX respectively.

From the TX coordinates, the coordinates of each scatterer of a cluster are computed by:

$$x_{c,s} = x^{TX} + a_c cos(\theta_{c,s}^{TX}) cos(\phi_{c,s}^{TX}) \quad (2)$$

$$y_{c,s} = y^{TX} - a_c cos(\theta_{c,s}^{TX}) sin(\phi_{c,s}^{TX}) \quad (3)$$

$$z_{c,s} = z^{TX} + a_c sin(\theta_{c,s}^{TX}) \quad (4)$$

The distance between each scatterer and the RIM is calculated as:

$$d_{c,s} = ((x^{RIM} - x^{c,s})^2 + (y^{RIM} - y^{c,s})^2 + (z^{RIM} - z^{c,s})^2)^{1/2} \quad (5)$$

Finally, the RIM arrival angles are obtained by:

$$\phi_{c,s}^{RIM} = I_\phi tan^{-1} \frac{|x^{RIM} - x^{c,s}|}{|y^{RIM} - y^{c,s}|} \quad (6)$$

with:

$$I_\phi = sgn(y^{c,s} - y^{RIM}) \quad (7)$$

$$\theta_{c,s}^{RIM} = I_\theta sin^{-1} \frac{|z^{RIM} - z^{c,s}|}{d_{c,s}} \quad (8)$$

where:

$$I_\theta = sgn(z^{c,s} - z^{RIM}) \quad (9)$$

From the RIM arrival angles $\theta_{c,s}^{RIM}$ of the signals reflected by the scatterers, that corresponds to the incidence angle on the metasurface, the values of electric field reflected by the metasurface are evaluated. They have been computed also considering different values for the amplitude of the signals reflected by the scatterers (from 0.01V/m to 1V/m, where the last one corresponds to the value of the transmitted signal from the base station). These values have been combined with the electric field generated for the incidence of the signal transmitted by the base station. The value of the electric fields have been computed through this formula:

$$E = \sum_{ii=1}^{m} \sum_{jj=1}^{n} A_{mn}\, e^{j\alpha_{mn}}\, cos(\theta_{mn})\, \|\Gamma_{ii,jj}\|\, cos(tt)\, e^{i<\Gamma_{ii,jj} + i\,k\,d\,\xi_{ii,jj}} \quad (10)$$

$$with \quad \xi_{\text{ii,jj}} = ((ii - \frac{1}{2})\cos(pp) + (jj - \frac{1}{2})\sin(pp))\sin(tt) \quad (11)$$

where *m* and *n* are the number of meta-atoms in the two dimensions, Γ is the reflection coefficient, *k* is the wavelength number and *d* is the distance among two adjacent meta-atoms (that corresponds to the length of a meta-atom, 3.81 mm). A_{mn} and α_{mn} are the amplitude and phase of the wave incident on the mn-th unit cell (set respectively to 1 and 0°), cos(θ,ϕ) is the scattering pattern of the mn-th unit cell (assuming meta-atoms as real-world dipolar scatterers), θ_{mn} corresponds to the incidence angle of the impinging signal that is measured from the perpendicular line to the metasurface. It has been set to 0°(orthogonal incidence) as regards the electric field component computed from the signal transmitted by the base station. *tt* and *pp* are two matrices made by the copy of two vectors θ and ϕ respectively in each row and in each column. More specifically, θ is a vector made by 100 equi-spaced values between 0 and $\frac{\pi}{2}$, while ϕ is made of the same number of values between 0 and 2π. The values of Γ are the ones evaluated for the meta-atom during the simulation.

To make the computations simpler and faster, the same arrival angle of the signals reflected by the scatterers of a cluster have been taken into account.

IV. Performance evaluation

In this section the performance of the system consisting of a base station, our designed reconfigurable intelligent metasurface and a mobile receiver are evaluated in presence of interferers between the base station and the metasurface.

The phase configurations computation of the metasurface performing beam-steering is based on a Genetic Algorithm (GA). This algorithm searches the phase configuration of the metasurface that allows to generate the radiation pattern with the direction of the main beam given in input to the algorithm and with a sidelobe level lower than 0.5. More details are reported in [4]. The maximum allowed S_{LL} has been set to 0.5 because the beam-width of the main beam is computed as HPBW (Half Power Beam-Width). In order to distinguish the main beam from the sidelobes, the sidelobe power should be lower than the half of the maximum power of the main beam. Moreover, we have considered the interval of angles 200°-340°for the azimuth ϕ angle, while the elevation angle θ remains fixed to 10°. That interval has been adopted for the

azimuth angles because our aim is tracking a mobile user who walks on the street and by putting the reconfigurable intelligent metasurface over a building facade, all the other angles cannot be used for tracking (for example at 90 °of azimuth angle the main beam would be directed towards the sky, that is not useful for our purpose).
The maximum sidelobe level of the radiation pattern generated by the metasurface and the angular deviations δ_θ and δ_ϕ of the main beam of the obtained radiation pattern have been evaluated for four different directions of the main beam, 225°, 260°, 315°and 340°. We consider a single cluster of 5/15/30 scatterers whose scattered signals impinge on the metasurface at a fixed angle 30°/50°/85°(table II). Two different amplitudes of the electric field of the scattered signals 0.1V/m and 0.5V/m have been taken into account. The deviations δ_θ and δ_ϕ have been evaluated between the output and the input and between the output and the output of the GA. As it is possible to notice from the fig. 4, the maximum SLL increases when the power and the number of the scatterers increases. Regarding the deviations of the angles of the main beam (fig.5,8 and 11), they don't have a specific trend wrt. the number and the power of the scatterers because the chosen phase configurations from the algorithm seem to be insensitive in terms of direction of the generated main beam. Concerning the configuration obtained for 340°, the deviations get worse increasing the number and the power of the scatterers.

TABLE II

angles of incidence	30°, 50°, 85°
number of scatterers	5, 15, 30
E field magnitudes of the scattered signals	0.1, 0.5

As expected, the sidelobe level increases by increasing the number of scatterers and their power. Moreover, the radiation patterns become worst in terms of SLL when the angle of incidence is increased from 30°to 85°, but certain radiation patterns (i.e., the one corresponding to 225°) becomes better passing from 30°to 50°. Also the accuracy of the adopted algorithm to compute the best phase configuration has been evaluated through the confusion matrices. They allow to evaluate the errors in terms of direction of the beam made by the algorithm in presence of interferers. Confusion matrices have been evaluated for each angle of incidence of the cluster of scatterers and for 5/15/30 scatterers and for two levels of scattered power (0.1 V/m and 0.5 V/m). Rows (w1-w7) contain the desired angles while columns (p1-p7) the obtained angles.

TABLE III

w1/p1	w2/p2	w3/p3	w4/p4	w5/p5	w6/p6	w7/p7
210°	230°	250°	270°	290°	310°	330°

In case of angle of incidence 30°(Tables 6 and 7), the accuracy is 57.14% independently from the number of scatterers. At 50°of angle of incidence (Tables 9 and 10), the accuracy gets worse with 0.5 V/m of magnitude of the electric field of the scatterers and with 30 scatterers (42.86%). When the angle of incidence is 85°(Tables 12 and 13), the accuracy gets better in certain cases. The different behaviour of the case of the 85°incident angle can be explained with the lower reflection coefficient amplitudes for 3 states (00, 01, 10), so the scattering signals are reflected less by the considered metasurface, and they affect less the main signal.

V. Conclusion

In this paper a wireless beam-steering system with a reconfigurable intelligent metasurface for outdoor environment has been presented. We have designed a new meta-atom structure and demonstrated its suitability for tracking purpose in terms of reflection coefficient. Then the channel model has been discussed considering a realistic scenario with scatterers between the transmitter and the RIM. A Genetic Algorithm (GA) has been adopted to find the optimal phase configurations, both in terms of phase and side lobe levels, of the metasurface to perform beam-steering. Finally the performances of the algorithm in presence of 5/15/30 scatterers have been evaluated in terms of deviations of the obtained main beam from the desired one, obtained sidelobe level and accuracy of the algorithm. The sidelobe level gets worse when the number of scatterers is increased and when their scattered power increases. Besides it gets worse increasing the angle of incidence of the signals scattered by the cluster. As regards the accuracy of the algorithm in presence of interferers, it has a better behaviour at 85°of incident angle that can be explained thanks to the lower reflection coefficient amplitudes. The adoption of the confusion matrices is useful to understand the errors and to perform the required corrections to improve the Genetic Algorithm.

References

[1] M. Di Renzo et al., "Smart Radio Environments Empowered by Reconfigurable Intelligent Surfaces: How It Works, State of Research, and The Road Ahead," in IEEE Journal on Selected Areas in Communications, vol. 38, no. 11, pp. 2450-2525, Nov. 2020, doi: 10.1109/JSAC.2020.3007211

[2] Di Renzo, M., Debbah, M., Phan-Huy, DT. et al. Smart radio environments empowered by reconfigurable AI meta-surfaces: an idea whose time has come. J Wireless Com Network 2019, 129 (2019). https://doi.org/10.1186/s13638-019-1438-9

[3] W. Tang et al., "Wireless communications with reconfigurable intelligent surface: Path loss modeling and experimental measurement," Nov. 2019. [Online]. Available: https://arxiv.org/abs/1911.05326

[4] Carola Rizza, Valeria Loscrí, Mohammad Parchin. Real-Time Beam steering in mmWave with Re- configurable Intelligent Meta-surfaces. IEEE Global Communications Conference, Dec 2021, Madrid, Spain.

[5] V. Jamali, A. M. Tulino, G. Fischer, R. Mller, and R. Schober, "Intelligent reflecting and transmitting surface aided millimeter wave massive MIMO," Sep. 2019. [Online]. Available: https://arxiv.org/abs/1902.07670

[6] J. Hey, H. Wymeersch, T. Sanguanpuaky, O. Silvenz, and M. Juntti, "Adaptive beamforming design for mmWave RIS-aided joint localization and communication," Nov. 2019. [Online]. Available: https://arxiv.org/abs/1911.02813

[7] X. Yang, C.-K. Wen, and S. Jin, "MIMO detection for reconfigurable intelligent surface-assisted millimeter wave systems," Apr. 2020. [Online]. Available: https://arxiv.org/abs/1902.07670

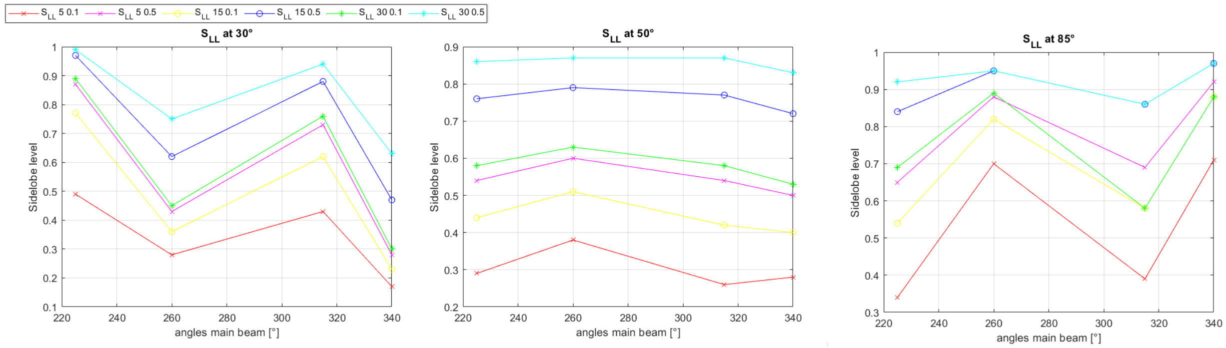

Fig. 4. S_{LL} at 30°, 50°and 85°angle of incidence of the cluster of scatterers.

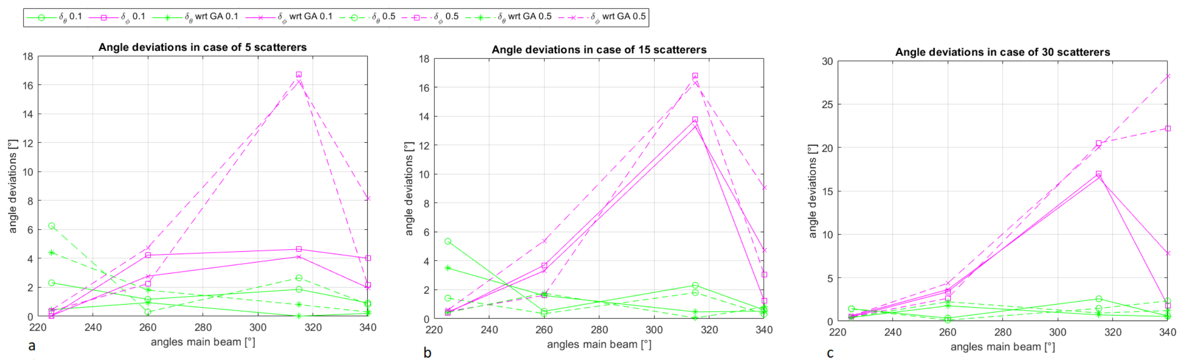

Fig. 5. Angle deviations with 30°angle of incidence of the cluster of scatterers.

Exp. w	p1	p2	p3	p4	p5	p6	p7
w1	0	1	0	0	0	0	0
w2	0	1	0	0	0	0	0
w3	0	0	1	0	0	0	0
w4	0	0	1	0	0	0	0
w5	0	0	0	0	0	1	0
w6	0	0	0	0	0	1	0
w7	0	0	0	0	0	0	1

Exp. w	p1	p2	p3	p4	p5	p6	p7
w1	0	1	0	0	0	0	0
w2	0	1	0	0	0	0	0
w3	0	0	1	0	0	0	0
w4	0	0	1	0	0	0	0
w5	0	0	0	0	0	1	0
w6	0	0	0	0	0	1	0
w7	0	0	0	0	0	0	1

Exp. w	p1	p2	p3	p4	p5	p6	p7
w1	0	1	0	0	0	0	0
w2	0	1	0	0	0	0	0
w3	0	0	1	0	0	0	0
w4	0	0	1	0	0	0	0
w5	0	0	0	0	0	1	0
w6	0	0	0	0	0	1	0
w7	0	0	0	0	0	0	1

Fig. 6. Confusion matrices with 30°angle of incidence, different number of scatterers (5, 15 and 30) and with 0.1 V/m for the amplitude of the scattered signals.

Exp. w	p1	p2	p3	p4	p5	p6	p7
w1	0	0	0	0	0	0	0
w2	0	1	0	0	0	0	0
w3	0	0	1	0	0	0	0
w4	0	0	1	0	0	0	0
w5	0	0	0	0	0	1	0
w6	0	0	0	0	0	1	0
w7	0	0	0	0	0	0	1

Exp. w	p1	p2	p3	p4	p5	p6	p7
w1	0	1	0	0	0	0	0
w2	0	1	0	0	0	0	0
w3	0	0	1	0	0	0	0
w4	0	0	1	0	0	0	0
w5	0	0	0	0	0	1	0
w6	0	0	0	0	0	1	0
w7	0	0	0	0	0	0	1

Exp. w	p1	p2	p3	p4	p5	p6	p7
w1	0	1	0	0	0	0	0
w2	0	1	0	0	0	0	0
w3	0	0	1	0	0	0	0
w4	0	0	1	0	0	0	0
w5	0	0	0	0	0	1	0
w6	0	0	0	0	0	1	0
w7	0	0	0	0	0	0	1

Fig. 7. Confusion matrices with 30°angle of incidence, different number of scatterers (5, 15 and 30) and with 0.5 V/m for the amplitude of the scattered signals.

[8] Basar, Ertugrul & Yıldırım, İbrahim. (2020). Indoor and Outdoor Physical Channel Modeling and Efficient Positioning for Reconfigurable Intelligent Surfaces in mmWave Bands. Available: https://doi.org/10.48550/arXiv.2006.02240

[9] Microwave Studio,"Computer Simulation Technology," 2017.

[10] I. A. Hemadeh, K. Satyanarayana, M. El-Hajjar and L. Hanzo, "Millimeter-Wave Communications: Physical Channel Models, Design Considerations, Antenna Constructions, and Link-Budget," in IEEE Communications Surveys & Tutorials, vol. 20, no. 2, pp. 870-913, 2017.

[11] M. K. Samimi and T. S. Rappaport, "Statistical channel model with multi-frequency and arbitrary antenna beamwidth for millimeter-wave outdoor communications," in 2015 IEEE Globecom Workshops (GC Wkshps), 2015, pp. 1–7.

[12] S. Buzzi and C. D'Andrea, "On clustered statistical MIMO millimeter wave channel simulation," Apr. 2016. [Online]. Available: arXiv:1604.00648

[13] O. E. Ayach, S. Rajagopal, S. Abu-Surra, Z. Pi, and R. W. Heath, "Spatially sparse precoding in millimeter wave MIMO systems," IEEE Trans. Wireless Commun., vol. 13, no. 3, pp. 1499–1513, Mar. 2014.

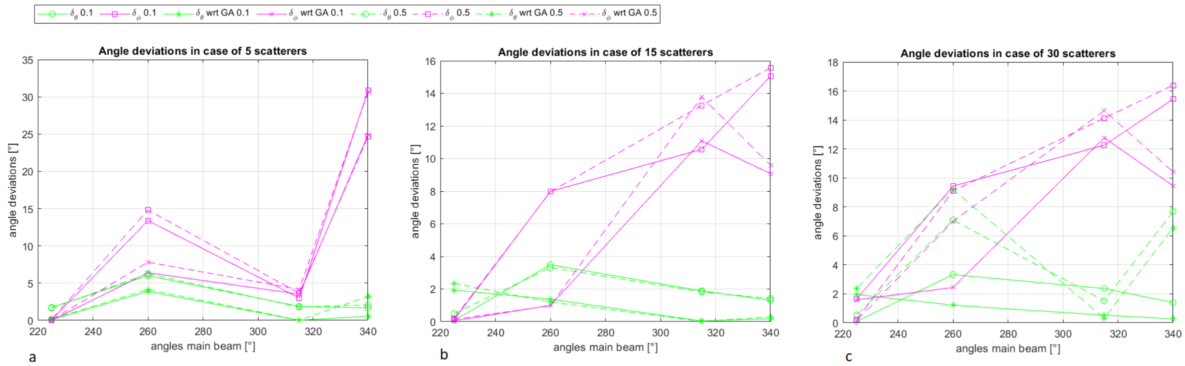

Fig. 8. Angle deviations with 50°angle of incidence of the cluster of scatterers.

Exp. w	p1	p2	p3	p4	p5	p6	p7
w1	0	1	0	0	0	0	0
w2	0	1	0	0	0	0	0
w3	0	0	1	0	0	0	0
w4	0	0	1	0	0	0	0
w5	0	0	0	0	0	1	0
w6	0	0	0	0	0	1	0
w7	0	0	0	0	0	0	1

Exp. w	p1	p2	p3	p4	p5	p6	p7
w1	0	1	0	0	0	0	0
w2	0	1	0	0	0	0	0
w3	0	0	1	0	0	0	0
w4	0	0	1	0	0	0	0
w5	0	0	0	0	0	1	0
w6	0	0	0	0	0	1	0
w7	0	0	0	0	0	0	1

Exp. w	p1	p2	p3	p4	p5	p6	p7
w1	0	1	0	0	0	0	0
w2	0	1	0	0	0	0	0
w3	0	0	1	0	0	0	0
w4	0	0	1	0	0	0	0
w5	0	0	0	0	0	0	1
w6	0	0	0	0	0	0	1
w7	0	0	0	0	0	0	1

Fig. 9. Confusion matrices with 50°angle of incidence, different number of scatterers (5, 15 and 30) and 0.1 V/m for the amplitude of the scattered signals.

Exp. w	p1	p2	p3	p4	p5	p6	p7
w1	0	1	0	0	0	0	0
w2	0	1	0	0	0	0	0
w3	0	0	1	0	0	0	0
w4	0	0	1	0	0	0	0
w5	0	0	0	0	0	0	1
w6	0	0	0	0	0	0	1
w7	0	0	0	0	0	0	1

Exp. w	p1	p2	p3	p4	p5	p6	p7
w1	0	1	0	0	0	0	0
w2	0	1	0	0	0	0	0
w3	0	0	1	0	0	0	0
w4	0	0	1	0	0	0	0
w5	0	0	0	0	0	0	1
w6	0	0	0	0	0	0	1
w7	0	0	0	0	0	0	1

Exp. w	p1	p2	p3	p4	p5	p6	p7
w1	0	1	0	0	0	0	0
w2	0	1	0	0	0	0	0
w3	0	0	1	0	0	0	0
w4	0	0	1	0	0	0	0
w5	0	0	0	0	0	0	1
w6	0	0	0	0	0	0	1
w7	0	0	0	0	0	0	1

Fig. 10. Confusion matrices with 50°angle of incidence, different number of scatterers (5, 15 and 30) and 0.5 V/m for the amplitude of the scattered signals.

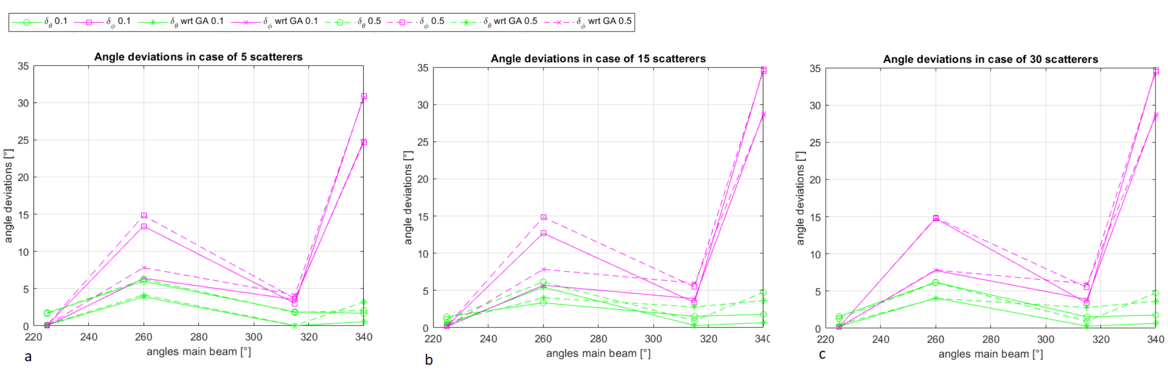

Fig. 11. Angle deviations with 85°angle of incidence of the cluster of scatterers.

Exp. w	p1	p2	p3	p4	p5	p6	p7
w1	0	1	0	0	0	0	0
w2	0	1	0	0	0	0	0
w3	0	0	1	0	0	0	0
w4	0	0	1	0	0	0	0
w5	0	0	0	0	0	1	0
w6	0	0	0	0	0	1	0
w7	0	0	0	0	0	0	1

Exp. w	p1	p2	p3	p4	p5	p6	p7
w1	0	1	0	0	0	0	0
w2	0	1	0	0	0	0	0
w3	0	0	1	0	0	0	0
w4	0	0	0	1	0	0	0
w5	0	0	0	0	0	1	0
w6	0	0	0	0	0	1	0
w7	0	0	0	0	0	0	1

Exp. w	p1	p2	p3	p4	p5	p6	p7
w1	0	1	0	0	0	0	0
w2	0	1	0	0	0	0	0
w3	0	0	1	0	0	0	0
w4	0	0	0	1	0	0	0
w5	0	0	0	0	0	1	0
w6	0	0	0	0	0	1	0
w7	0	0	0	0	0	0	1

Fig. 12. Confusion matrices with 85°angle of incidence, different number of scatterers (5, 15 and 30) and 0.1 V/m for the amplitude of the scattered signals.

Exp. w	p1	p2	p3	p4	p5	p6	p7
w1	0	1	0	0	0	0	0
w2	0	1	0	0	0	0	0
w3	0	0	1	0	0	0	0
w4	0	0	0	1	0	0	0
w5	0	0	0	0	0	1	0
w6	0	0	0	0	0	1	0
w7	0	0	0	0	0	0	1

Exp. w	p1	p2	p3	p4	p5	p6	p7
w1	0	1	0	0	0	0	0
w2	0	1	0	0	0	0	0
w3	0	0	1	0	0	0	0
w4	0	0	0	1	0	0	0
w5	0	0	0	0	0	1	0
w6	0	0	0	0	0	1	0
w7	0	0	0	0	0	1	0

Exp. w	p1	p2	p3	p4	p5	p6	p7
w1	0	1	0	0	0	0	0
w2	0	1	0	0	0	0	0
w3	0	0	1	0	0	0	0
w4	0	0	0	1	0	0	0
w5	0	0	0	0	0	1	0
w6	0	0	0	0	0	1	0
w7	0	0	0	0	0	1	0

Fig. 13. Confusion matrices with 85°angle of incidence, different number of scatterers (5, 15 and 30) and 0.5 V/m for the amplitude of the scattered signals.